J Mater Sci (2010) 45:39–45
DOI 10.1007/s10853-009-3881-1

Effect of process parameters on stir zone microstructure in Ti–6Al–4V friction stir welds

L. Zhou · H. J. Liu · Q. W. Liu

Received: 9 June 2009 / Accepted: 11 September 2009 / Published online: 26 September 2009

Abstract The effects of the main process variables on the stir zone microstructure in friction stir welds were investigated for Ti–6Al–4V. Welds were produced by employing varying welding speeds under a constant rotation speed or different rotation speeds at a constant welding speed. The stir zone microstructure was examined by optical microscopy and transmission electron microscopy. It was found that the stir zone microstructure was determined by the parameters controlling temperature and deformation history during the friction stir welding. A bimodal microstructure characterized by primary α and transformed β with lamellar $\alpha + \beta$ or a full lamellar microstructure composed of basket-weave $\alpha + \beta$ lamellae could be developed in the stir zone. The microstructural evolution mechanism in the stir zone was discussed.

Introduction

Titanium and its alloys have high specific strength and excellent corrosion resistance, and thus have been extensively applied in the aerospace, chemical and nuclear industries. Since the introduction of titanium and titanium alloys in the early 1950s, Ti–6Al–4V has in a relatively short time become the most widely used titanium alloy due to its excellent comprehensive properties [1]. In recent years, the demand for Ti–6Al–4V is increasing due to the scarcity of resources and their growing expense especially in the aerospace sector. Almost all conventional welding technologies have been applied to join Ti–6Al–4V. However, the application of fusion welding techniques to Ti–6Al–4V resulted in formation of brittle coarse microstructure, severe distortion and high residual stress. Therefore, solid-state joining processes would appear to be more suitable for avoiding the problems associated with the melting of the materials to be welded.

Friction stir welding (FSW) has attracted a great deal of attention in the industrial fields due to its many advantages. Since its invention in 1991, FSW has been successfully applied to the joining of the various Al, Mg and Cu alloys [2–6]. In recent years, friction stir welding of high melting temperature materials such as steels, nickel and titanium alloys has become a research hotspot [7–9]. However, FSW of high melting temperature materials is difficult to create sound joint because of tool limitations [10, 11].

Until now, there has been limited information in the archival literature regarding the FSW of titanium alloys, and thus the microstructural development in the FSW welds of titanium alloys is still not well understood [12–25]. Therefore, the $\alpha + \beta$ titanium alloy, Ti–6Al–4V, is friction stir welded by a W-Re pin tool in the present paper, and the microstructural evolution in the stir zone (SZ) is studied to reveal the relation between microstructure and process parameters.

Experimental procedure

The as-received material was 2-mm-thick mill-annealed Ti–6Al–4V sheet with the chemical composition of Al 6.15, V 4.00, Fe 0.30, C 0.10, N 0.05, H 0.015, O 0.20 and

L. Zhou · H. J. Liu (✉) · Q. W. Liu
State Key Laboratory of Advanced Welding Production Technology, Harbin Institute of Technology, Harbin 150001, People's Republic of China
e-mail: liuhj@hit.edu.cn

L. Zhou
e-mail: hitalimse@gmail.com

Ti balance (wt%). Welding experiments were performed using a special welding system equipped with a W-Re pin tool designed by the Harbin Institute of Technology, P.R. China. The pin tool used in the present study was conical shape. The tool shoulder diameter was 11 mm; the pin length was 1.8 mm and the pin was tapered from 6 mm at the shoulder to 4 mm at the pin tip. Welds were made along the longitudinal direction of the sheet (perpendicular to the rolling direction of the sheet) with welding speeds of 25, 50 and 100 mm/min at a constant rotation speed of 400 rpm or with rotation speeds of 400, 500 and 600 rpm under a constant welding speed of 75 mm/min. A 2.5° tilt was applied to the pin tool for all the welding experiments.

The transverse weld cross-sections were cut by electrical discharge machining and prepared by standard metallographic procedure. Samples were mounted in epoxy and ground with abrasive paper. The microstructures were observed by optical microscopy (OM) and transmission electron microscopy (TEM). The polished weld cross-sections were chemically etched using Kroll's reagent (13 mL HF, 26 mL HNO_3 and 100 mL H_2O) and then observed on an Olympus-PMG3 OM. Thin-foil disk specimens were cut from the SZ for the TEM observation. The specimens were first mechanically polished to a thickness of 0.1 mm and then twin-jet electro-polished in a solution (6 vol.% $HClO_4$ + 34 vol.% C_4H_9OH + 60 vol.% CH_3OH) at −40 °C. TEM observations were performed on a Philips CM-12 microscope operated at an accelerating voltage of 120 kV.

Results and discussion

Features of the microstructural zones

A typical cross-section of the Ti–6Al–4V friction stir weld is shown in Fig. 1a. The thermo-mechanically affected zone (TMAZ) is not found outside the SZ on either advancing side or retreating side, thus the weld only consists of SZ, instead of SZ + TMAZ. The absence of TMAZ in titanium alloy FSW welds has also been reported in references [20–22]. The SZ is clearly visible around the weld center. The sideward lighter zone is the base material (BM), and the narrow gray zone between the SZ and the BM is the heat affected zone (HAZ). A full penetration weld is obtained and the weld thickness is slightly smaller than the BM. The weld cross-section looks like 'basin-shape' and process parameters have little influence on the weld cross-section appearance. No volumetric defect is observed in the cross-section of any of the welds.

Optical micrograph of the BM is shown in Fig. 1b. The BM has an initial microstructure characterized by elongated primary α + transformed β. It is indicated that the BM is rolled in the $\alpha + \beta$ temperature range, and then annealed below the β-transus temperature followed by air cooling. The white and grey regions in the OM image represent primary α and transformed β, respectively.

The shape of the HAZ is influenced by the process parameters. However, temperature in the HAZ is below the

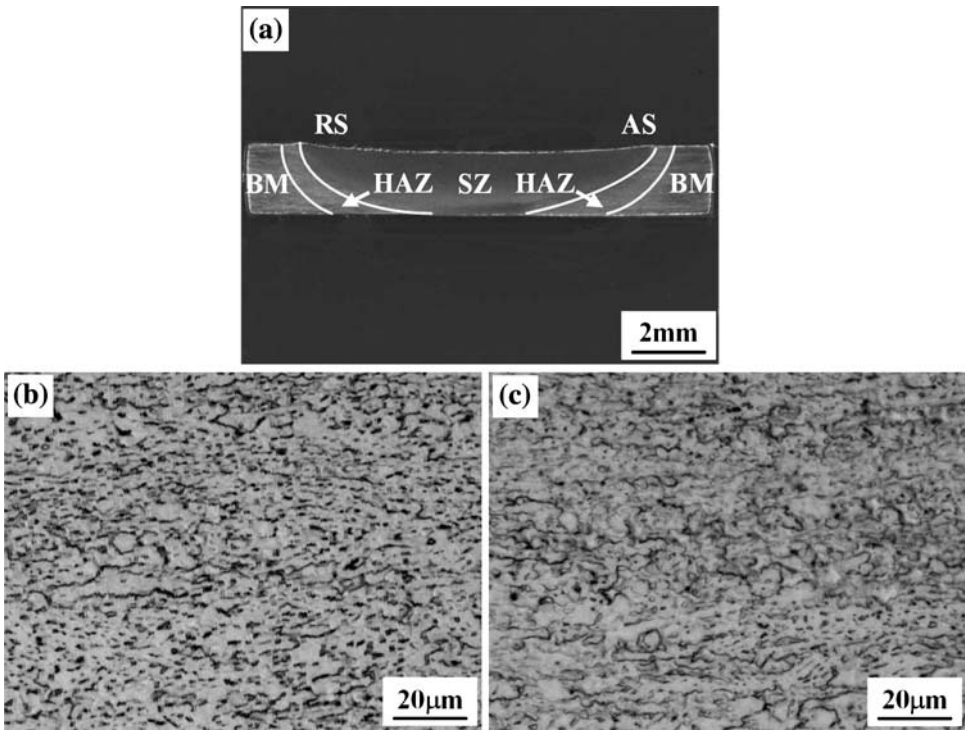

Fig. 1 Optical micrographs of **a** weld cross-section, **b** BM and **c** HAZ

β-transus temperature for any of the welds, and thus there is little difference in the HAZ microstructure between welds obtained with varying parameters. A typical optical micrograph of the HAZ is shown in Fig. 1c. The microstructure of the HAZ is similar to that of the BM but with an increase in the volume fraction of β, which can be explained by the $\alpha \rightarrow \beta$ transformation in this region during the heating stage of FSW. However, high-temperature residence time in the HAZ is relatively short so the increase in the volume fraction of β is not significant.

Microstructure of the SZ

The SZ microstructure in the weld is significantly influenced by the process parameters. The effects of welding speed and rotation speed are discussed, respectively.

Effect of welding speed on the SZ microstructure

Figure 2 shows the effect of welding speed on the SZ microstructure in the welds produced at a constant rotation speed of 400 rpm. The SZ microstructure in all the welds is characterized by primary α + transformed β. This means the maximum temperature in the SZ does not exceed the β-transus temperature. The details of the transformed β in the SZ cannot be revealed by OM due to the quite fine microstructure.

Primary α grain size is an important factor affecting the mechanical properties of titanium alloys [26]. As seen in Fig. 2, the mean size of primary α in the SZ increases with increasing welding speed. For welding speeds of 25 and 50 mm/min, primary α size in the SZ is much finer than that in the BM. When welding speed rises to 75 and 100 mm/min, primary α size in the SZ is gradually close to that in the BM. The size of primary α as a function of welding speed in the welds made at 400 rpm is shown in Fig. 2d. With increasing welding speed, primary α size increases from 2 to 11 μm.

Effect of rotation speed on the SZ microstructure

Figure 3 shows the effect of rotation speed on the SZ microstructure in the welds produced at a constant welding speed of 75 mm/min. The SZ is composed of primary α + transformed β when a rotation speed of 400 rpm is adopted. It can be concluded that the peak temperature in the SZ of the weld produced at 400 rpm is also below the β-transus temperature. However, the SZ is characterized by a full lamellar microstructure when the rotation speeds of 500 and 600 rpm are used. It is suggested that the SZ temperature is above the β-transus temperature, and thus a full lamellar microstructure is formed during cooling from the β-field [27].

The lamellar microstructure in the welds produced at 500 and 600 rpm is obvious, as shown in Fig. 3. Prior β grain size increases with increasing rotation speed. This phenomenon is attributed to prior β grain growth when higher rotation speeds are applied. It is well known that

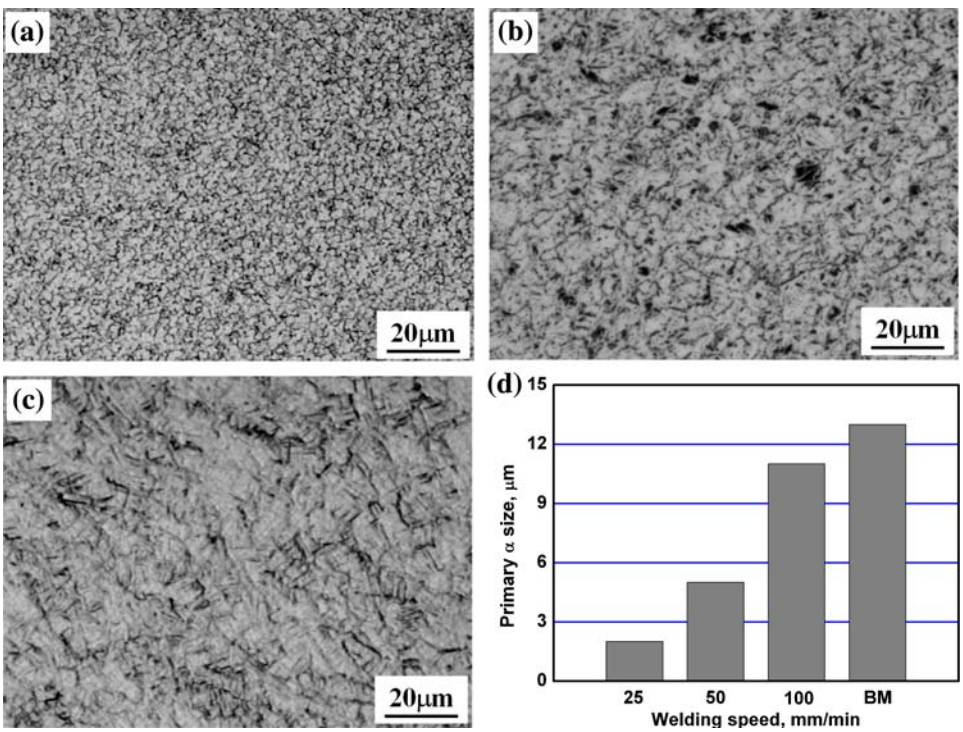

Fig. 2 Optical micrographs of the SZ in the welds produced at a constant rotation speed of 400 rpm: **a** 25 mm/min, **b** 50 mm/min, **c** 100 mm/min and **d** primary α size as a function of welding speed

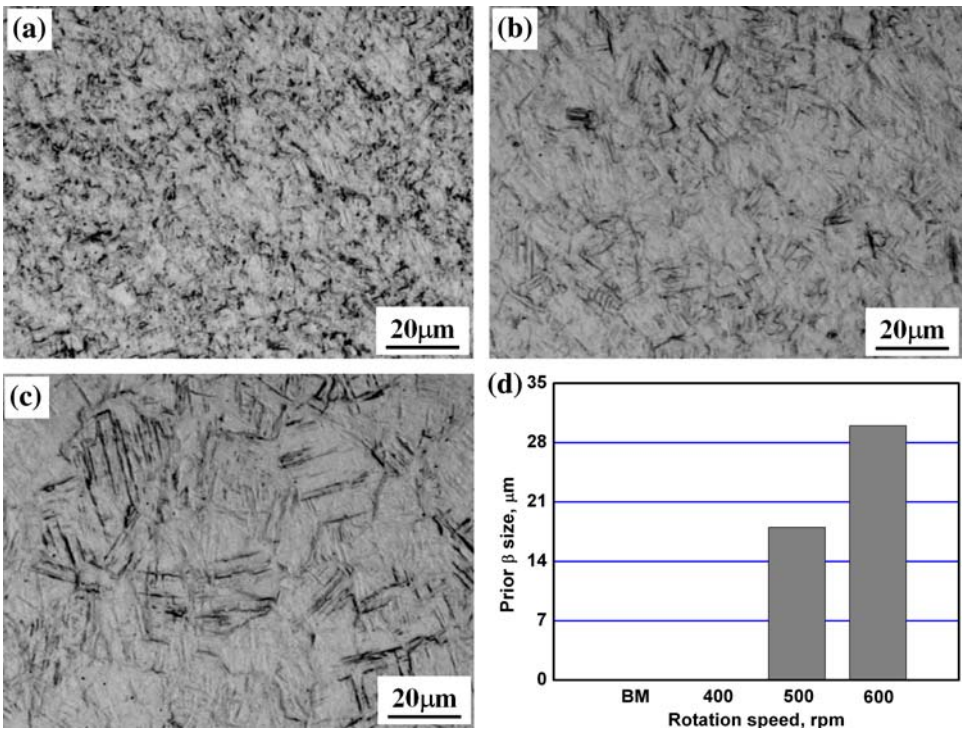

Fig. 3 Optical micrographs of the SZ in the welds produced at a constant welding speed of 75 mm/min: **a** 400 rpm, **b** 500 rpm, **c** 600 rpm and **d** primary β size as a function of rotation speed

higher rotation speed would cause a higher peak temperature and a longer dwell time above the β-transus temperature in the SZ, which results in coarser prior β grains [28]. The size of prior β as a function of rotation speed in the welds made at 75 mm/min is shown in Fig. 3d. Since the as-received material and the weld for 400 rpm are processed below the β-transus, only prior β size in the welds produced at 500 and 600 rpm is given.

Evolution mechanism of the SZ microstructure

The evolution mechanism of the SZ microstructure is further revealed by TEM. In the present study, two kinds of welds are examined. One is the welds for the welding speeds of 25 and 100 mm/min at a constant rotation speed of 400 rpm, and another is the welds for the rotation speeds of 400 and 600 rpm at a constant welding speed of 75 mm/min.

Effect of welding speed on the evolution mechanism

Figure 4 shows the TEM images of the SZ in the weld for 400 rpm and 25 mm/min. The SZ is characterized by dislocation-free equiaxed primary α and transformed β with lamellar $\alpha + \beta$, thus the microstructure in the SZ can be defined as a bimodal microstructure. The existence of dislocation-free equiaxed α indicates that fully dynamic recrystallization (DRX) occurs in the SZ [29]. The temperature in the SZ is close to the β-transus temperature, thus $\alpha \rightarrow \beta$ transformation occurs during the heating stage of the welding process. During the cooling stage of FSW, $\beta \rightarrow \alpha + \beta$ transformation occurs and alternate lamellar $\alpha + \beta$ is formed. The selected area electron diffraction (SAED) patterns have confirmed the existence of the alternate α and β phase in the lamellar microstructure, as shown in Fig. 4.

The microstructure of the SZ in the weld for 400 rpm and 100 mm/min is also a bimodal microstructure, as shown in Fig. 5. However, there exists some difference in detailed microstructure. Unlike the weld for 400 rpm and 25 mm/min, there are considerable amount of fine subgrains within primary α as well as DRX α in the SZ, as shown in Fig. 5a. This phenomenon indicates that the DRX process is not fully developed in the SZ of the weld for 400 rpm and 100 mm/min.

As mentioned above, primary α size in the SZ increases with increasing welding speed when a constant rotation speed of 400 rpm is adopted. It has been reported in Al alloy FSW welds that the mean grain size in the SZ decreases with increasing welding speed for a given rotation speed [30, 31]. The FSW performed at higher tool rotation speed or higher ratio of rotation speed/welding speed results in an increase in both the degree of deformation and the peak temperature of thermal cycle. The increase in the degree of deformation during FSW results in a reduction in the recrystallized grain size according to the general principles for recrystallization [29]. The effect of deformation may be more obvious on the SZ microstructure for the welds

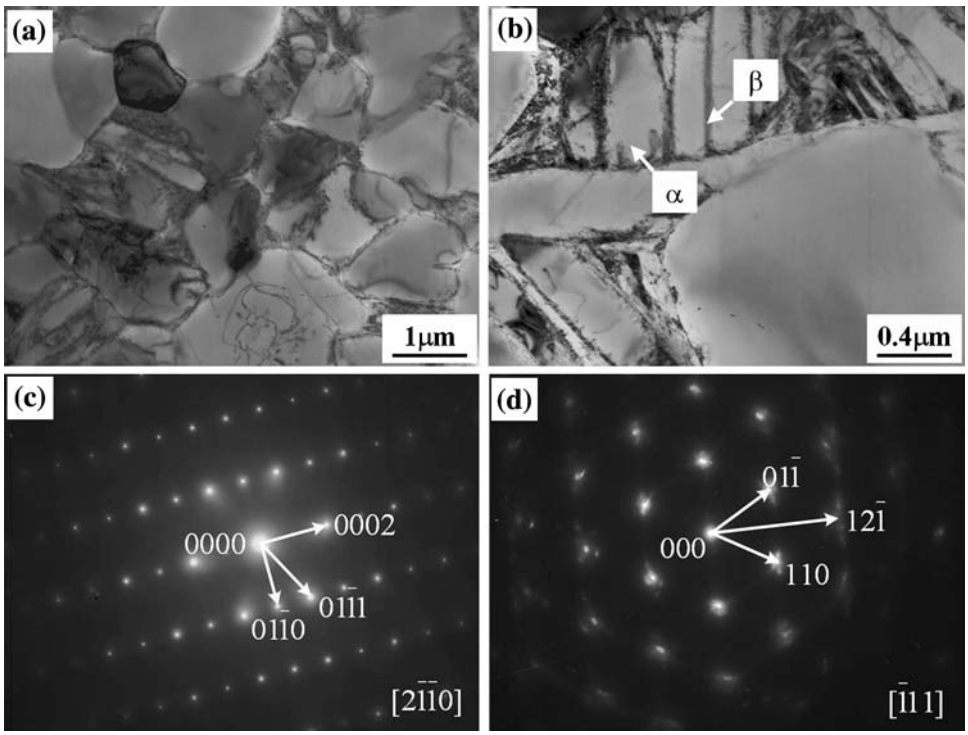

Fig. 4 TEM images of SZ in the weld for 400 rpm and 25 mm/min: **a** DRX α, **b** lamellar α + β, **c** SAED pattern of α phase and **d** SAED pattern of β phase

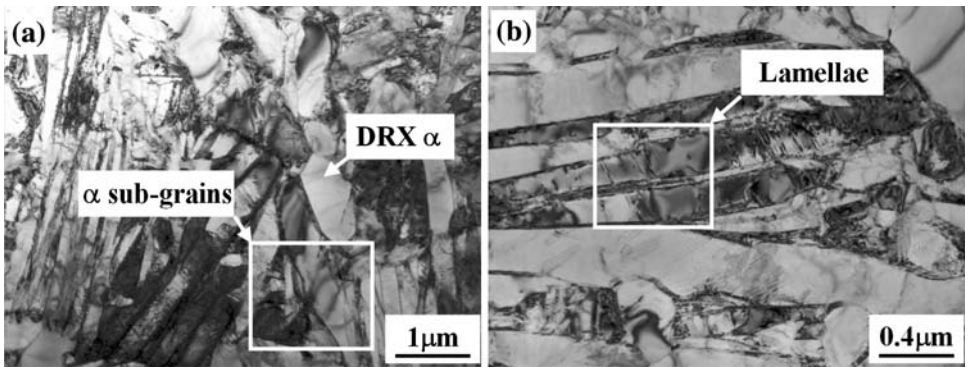

Fig. 5 TEM images of SZ in the weld for 400 rpm and 100 mm/min: **a** DRX α and α sub-grains and **b** α + β lamellae

produced at a constant rotation speed of 400 rpm when lower welding speeds are used. That is the reason why DRX is not fully developed and primary α size in the SZ increases with increasing welding speed.

Compared with the weld for 400 rpm and 25 mm/min, fine lamellae are formed in transformed β in the SZ of the weld for 400 rpm and 100 mm/min, as shown in Fig. 5b. It is known that β would transform to finer lamellar microstructure at a higher cooling rate. This is thought to be the reason why the higher welding speed leads to a decrease in lamellae width.

Effect of rotation speed on evolution mechanism

The discussion of the effect of rotation speed on the SZ microstructure evolution in the welds produced at a constant welding speed of 75 mm/min is focused on the welds for the rotation speeds of 400 and 600 rpm at a constant welding speed of 75 mm/min.

A full lamellar microstructure is developed within prior β grains in the weld for 600 rpm and 75 mm/min, as seen in Fig. 6a. Unlike the parallel α + β lamellae in the weld for 400 rpm and 75 mm/min, basket-weave α + β lamellae are formed in the weld for 600 rpm and 75 mm/min. It is well-known that the corresponding transformation of the slip planes of the body-centered cubic β titanium into the basal planes of the close-packed hexagonal α titanium and the respective orientations of the slip directions are given by the orientation relationship: $\{0001\}_\alpha // \{110\}_\beta$ and $\langle 1120\rangle_\alpha // \langle 111\rangle_\beta$. The six slip planes and the two slip directions of the β titanium unit cell give a maximum of 12 variants of orientation to the α. Consequently, this results in

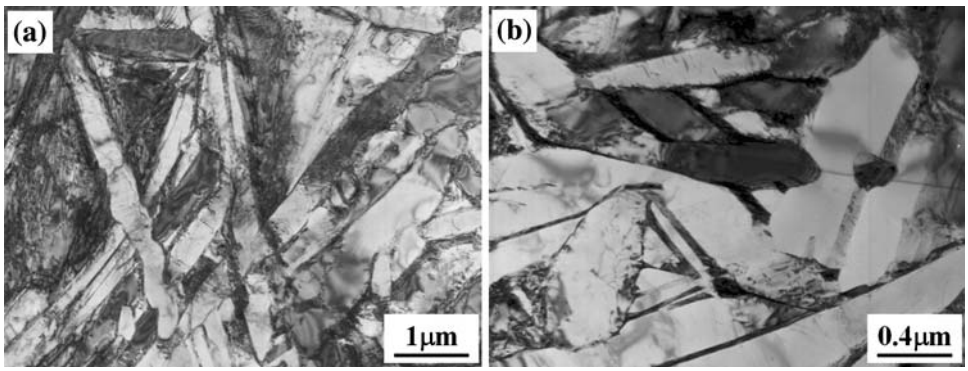

Fig. 6 TEM images of SZ in the weld for 600 rpm and 75 mm/min: **a** basket-weave lamellar $\alpha + \beta$ and **b** low dislocation density α lamellae

a very characteristic microstructure similar in appearance to the weave pattern of a basket and is therefore referred to as basket-weave structure [27].

A higher magnification of the basket-weave $\alpha + \beta$ lamellae is shown in Fig. 6b. It is interesting to note that the SZ contains dislocation-free colony α as well as α colonies with low dislocation density in the weld for 600 rpm and 75 mm/min. This observation agrees with the results of Juhas et al. [25]. However, randomly oriented twins and a high dislocation density in the Ti–6Al–4V FSW welds have been reported in references [17, 24]. It can be argued that the dislocation density within the grains must be dependent on process parameters. As for the parameters used in the present study, the material behind the tool can still be above the β-transus temperature when it is no longer being deformed and thus experiences no deformation as it cools below the β-transus temperature, and thus dislocation-free colony α as well as α colonies with low dislocation density are developed.

Conclusions

The $\alpha + \beta$ titanium alloy, Ti–6Al–4V, was friction stir welded using different welding speeds and different rotation speeds and then microstructural evolution of the SZ was examined. The SZ microstructure was determined by the process parameters controlling temperature and deformation history. For the weld produced at the constant rotation speed of 400 rpm, the SZ temperature was below the β-transus temperature and a bimodal microstructure characterized by primary α + transformed β with lamellar $\alpha + \beta$ was formed in the SZ due to DRX, and primary α size increased but the lamellae width in transformed β decreased with increasing welding speed from 25 to 100 mm/min because of the comprehensive action of deformation extent and cooling rate. For the welds produced at a constant welding speed of 75 mm/min, the SZ temperature was below the β-transus temperature when a rotation speed of 400 rpm was used and the microstructure in the SZ was also a bimodal microstructure, while the SZ temperature was above the β-transus temperature when rotation speeds of 500 and 600 rpm were used, and thus a full lamellar microstructure characterized by basket-weave $\alpha + \beta$ lamellae was developed in the SZ.

Acknowledgements The research was sponsored by the National Key Technology Research and Development Program No. 2006BAF04B09, Ministry of Science and Technology, P.R. China, and was supported by the Program of Excellent Team in Harbin Institute of Technology, P.R. China.

References

1. Polmear IJ (1996) Mater Trans JIM 37:12
2. Venkateswaran P, Xu ZH, Li XD, Reynolds AP (2009) J Mater Sci 44:4140. doi:10.1007/s10853-009-3607-4
3. Chen T (2009) J Mater Sci 44:2573. doi:10.1007/s10853-009-3336-8
4. Lee CY, Lee WB, Kim JW, Choi DH, Yeon YM, Jung SB (2008) J Mater Sci 43:3296. doi:10.1007/s10853-008-2525-1
5. Gerlich A, Yamamoto M, North TH (2008) J Mater Sci 43:2. doi:10.1007/s10853-007-1791-7
6. Zhang Z, Chen JT (2008) J Mater Sci 43:222. doi:10.1007/s10853-007-2129-1
7. Mishra RS, Ma ZY (2005) Mater Sci Eng R 50:1
8. Nandan R, DebRoy T, Bhadeshia H (2008) Prog Mater Sci 53:980
9. Bhadeshia H, DebRoy T (2009) Sci Technol Weld Join 14:193
10. Gan W, Li ZT, Khurana S (2007) Sci Technol Weld Join 12:610
11. Lienert TJ, Stellwag WL, Grimmett BB, Warke RW (2003) Weld J 82:1
12. Pilchak AL, Juhas MC, Williams JC (2007) Metall Mater Trans A 38:435
13. Reynolds AP, Hood E, Tang W (2005) Scr Mater 52:491
14. Pilchak AL, Juhas MC, Williams JC (2007) Metall Mater Trans A 38:401
15. Mironov S, Zhang Y, Sato YS, Kokawa H (2008) Scr Mater 59:27
16. Mironov S, Zhang Y, Sato YS, Kokawa H (2008) Scr Mater 59:511
17. Pilchak AL, Norfleet DM, Juhas MC, Williams JC (2008) Metall Mater Trans A 39:1519
18. Sanders DG, Ramulu M, Edwards PD (2008) Materialwiss Werkstofftech 39:353
19. Sanders DG, Ramulu M, Klock-McCook EJ, Edwards PD, Reynolds AP, Trapp T (2008) J Mater Eng Perform 17:187

20. Lee WB, Lee CY, Chang WS, Yeon YM, Jung SB (2005) Mater Lett 59:3315
21. Zhang Y, Sato YS, Kokawa H, Park SHC, Hirano S (2008) Mater Sci Eng A 488:25
22. Zhang Y, Sato YS, Kokawa H, Park SHC, Hirano S (2008) Mater Sci Eng A 485:448
23. Ramirez AJ, Juhas MC (2003) Mater Sci Forum 426–432:2999
24. Lienert TJ, Jata KV, Wheeler R, Seetharaman V (2001) Proceedings of joining of advanced and specialty materials III. ASM International, Materials Park
25. Juhas MC, Viswanathan GB, Fraser HL (2001) Proceedings of lightweight alloys for aerospace application. TMS, Warrendale
26. Lüjering G (1998) Mater Sci Eng A 243:32
27. Leyens C, Peters M (2003) Titanium and titanium alloys. Wiley-VCH, Cologne
28. Ding R, Guo Z, Wilson A (2002) Mater Sci Eng A 327:233
29. Humphreys FJ, Hatherly M (2004) Recrystallization and related annealing phenomena, 2nd edn. Elsevier, Amsterdam
30. Hassan AA, Prangnell PB, Norman AF, Price DA, Williams SW (2003) Sci Technol Weld Join 8:257
31. Cavaliere P, Squillace A, Panella F (2008) J Mater Process Technol 200:364